International Journal of Numerical Methods for Heat & Fluid Flow

Fluid-structure interaction analysis of buoyancy-driven fluid and heat transfer through an enclosure with a flexible thin partition

H. Zargartalebi, M. Ghalambaz, A. Chamkha, Ioan Pop, Amir Sanati Nezhad,

Received 11 September 2017
Revised 23 November 2017
Accepted 23 November 2017

Fluid-structure interaction analysis of buoyancy-driven fluid and heat transfer through an enclosure with a flexible thin partition

H. Zargartalebi
Department of Mechanical and Manufacturing Engineering, Centre for Bioengineering Research and Education, University of Calgary, Calgary, Canada

M. Ghalambaz
Department of Mechanical Engineering, Islamic Azad University, Dezful, Iran

A. Chamkha
Department of Mechanical Engineering, Prince Mohammad Bin Fahd University, Al-Khobar, Saudi Arabia and RAK Research and Innovation Center, American University of Ras Al Khaimah, Ras Al Khaimah, UAE

Ioan Pop
Department of Applied Mathematics, Babes-Bolyai University, Cluj-Napoca, Romania, and

Amir Sanati Nezhad
Department of Mechanical and Manufacturing Engineering, Centre for Bioengineering Research and Education, University of Calgary, Calgary, Canada

Abstract

Purpose – A numerical model of an unsteady laminar free convection flow and heat transfer is studied in a cavity that comprises a vertical flexible thin partition.

Design/methodology/approach – The left and right vertical boundaries are isothermal, while the horizontal boundaries are insulated. Moreover, the thin partition, placed in the geometric centerline of the enclosure, is considered to be hyper elastic and diathermal. Galerkin finite-element methods, the system of partial differential equations along with the appropriate boundary conditions are transformed to a weak form through the fluid-structure interaction and solved numerically.

Findings – The heat transfer characteristics of the enclosure with rigid and flexible partitions are compared. The effect of Rayleigh number and Young's modulus on the maximum nondimensional stress and final deformed shape of the membrane is addressed.

The work of I. Pop has been supported from the grant PN-III-P4-ID-PCE-2016-0036, UEFISCDI, Romania.

International Journal of Numerical Methods for Heat & Fluid Flow
Vol. 28 No. 9, 2018
pp. 2072-2088

0961-5539
DOI 10.1108/HFF-09-2017-0348

Originality/value – Incorporation of vertical thin flexible membrane in middle of a cavity has numerous industrial applications, and it could noticeably affect the heat and mass transfer in the enclosure.

Keywords Fluid-structure interaction, Flexible thin partition, Lagrangian–Eulerian formulation, Unsteady free convection

Paper type Research paper

Nomenclature

Latin symbols

d = Nondimensional displacement;
E = Young's modulus;
E_τ = Dimensionless Young's modulus;
f_i = Dimensionless body force introduced in equation (2);
F_v = Dimensionless body force introduced in equation (9);
g = Gravitational acceleration vector;
L = Cavity size;
p = Dimensionless pressure;
Pr = Prandtl number;
Ra = Thermal Rayleigh number;
t = Dimensionless time;
T = Temperature;
T_O = Initial average of the temperature in the enclosure;
u = Dimensionless velocity vector;
u_p = Moving coordinate velocity;
W_s = Strain energy density function; and
x,y = Cartesian coordinates.

Greek symbols

α = Thermal diffusivity;
β = Thermal expansion coefficient;
ε = Strain;
ν = Kinematic viscosity;
θ = Nondimensional temperature;
ρ = Density;
σ = Stress tensor;
τ = Nondimensional time; and
υ = Poisson's ratio.

Subscripts

c = Cold;
f = Fluid;
h = Hot;
p = Partition; and
s = Solid.

Superscripts

* = Dimensional.

1. Introduction

Natural convection in a cavity is an enthralling engineering topic because of its broad applications in nature and engineering, e.g. electronic geothermal systems, chemical catalytic reactors, component cooling, thermal design of buildings, cryogenic storage and solar collector design (Sheremet and Pop, 2014; Martyushev and Sheremet, 2014). Most studies are dedicated to flow and heat transfer in an enclosure without partitions. Indeed, different realms of heat transfer have been studied in cavities such as conjugate heat transfer and nanofluids (Sheremet and Pop, 2014) or cavities with wavy walls (Sheremet and Pop, 2015; Sheikholeslami and Shamlooei, 2017), with internal radiation (Martyushev and Sheremet, 2014; Sheikholeslami and Shehzad, 2017a) and under different magnetic field (Sheikholeslami and Rashidi, 2015; Sheikholeslami and Shehzad, 2017b; Sheikholeslami *et al.*, 2017) and porous media conditions (Sheremet *et al.*, 2015). Nevertheless, there exist numerous investigations on the effect of vertical plate in the rectangular and triangular cavities useful for enhancing the free convection (Chamkha *et al.*, 2012; Sathiyamoorthy and Chamkha, 2014; Xu *et al.*, 2009; Saha *et al.*, 2014; Saha and Gu, 2014). Xu *et al.* (2009) studied the couple thermal boundary layer adjacent to the partition in a differentially-heated cavity. Saha and Gu (2014) investigated the heat transfer in an isosceles triangular enclosure partitioned in the center by an infinite conductive vertical wall. They showed the unsteady characteristics of the couple thermal boundary layers and the overall free convection flow in the partitioned triangular cavity. The unsteady behavior is more problematic for multifarious bases. Knowing the overall heat transfer rate across windows and walls that splitting up a hot room from a cold environment or vice versa, could help to optimize the building design. Furthermore, it is also essential to find out the interaction of two convective systems and partially conducting wall.

The previous studies have shown that the natural convection for the laminar flow regime dwindles with respect to a non-partitioned enclosure even when a perfectly conductive partition is used. Consequently, the heat transfer through the enclosure is noticeably descended (Xu *et al.*, 2009; Nishimura *et al.*, 1988; Duxbury, 1979; Cuckovic-Dzodzo *et al.*, 1999). Furthermore, all investigations are constrained to the rigid and fixed walls and partitions. On the other hand, several works accounted the effect of moving boundaries on the transport phenomena (Ralph and Pedley, 1988; Nakamura *et al.*, 2000; Nakamura *et al.*, 2001; Khaled and Vafai, 2002, 2003). For instance, Nakamura *et al.* (2001) study the effect of wall vibration on different features of heat and mass transfer in a channel, where the coordinate transformation method was used to change the flexible boundary into a fixed boundary problem. Some other studies evaluated the influence of the flexible bottom surface in an enclosure using fluid-structure interaction approach (Küttler and Wall 2008; Mehryan *et al.*, 2017; Al-Amiri and Khanafer, 2011). Al-Amiri and Khanafer (2011) considered the bottom wall as a flexible boundary and used fluid-structure interaction (FSI) analysis to study steady mixed convection heat transfer in a lid-driven enclosure.

The natural convection heat transfer in an enclosure containing chemical components is common phenomena. Enclosures are divided into sub enclosures by partition membranes, avoiding the mixing of chemical components. The coupling of the natural convection heat transfer flow with its interactions with a partition membrane is a new area of interest that is studied neither in the context of FSI problems nor the heat transfer problems. In a recent study, Jamesahar *et al.* (2016) focused on the unsteady natural convection in an enclosure separated by two triangles using a flexible thermal conductive partition. In this study, adopting an unstructured grid and a Lagrangian–Eulerian formulation, the impact of different important parameters on heat transfer was investigated.

Incorporation of a vertical thin flexible partition has not been reported yet, although it has multifarious industrial applications and could significantly affect the heat and mass transfer in the enclosure. Hence, in this study, for the first time, we address the steady

laminar free convection heat transfer in an enclosure compartmentalized with a flexible thin partition. The heat transfer behavior, the partition deflection and the induced maximum stress in the partition will be then investigated.

2. Mathematical formulation

A two-dimensional unsteady free convection in an enclosure including a vertical flexible wall is modeled. It is presumed that the left vertical wall is suddenly cooled down to Tc and the right vertical wall is suddenly heated up to T_h, where $T_h > T_c$. The bottom and top horizontal walls are insulated. The impermeable cavity walls are assumed to be non-conducting and rigid. In addition, two small vertical parts with the length 0.1 per cent of the height of cavity are considered to be open boundaries with relative pressure of zero to allow transportation of fluid owing largely to fluctuating of the flexible partition and consequently, the alteration of volume in each cavity part. In other words, as we have assumed that the fluid is incompressible, the deformation of the flexible partition changes the volume of each part of cavity and to have a mass conservation we need to assume these two open boundaries and due to the fact that these boundaries are really small, their presence near the top corners does not affect the solution. Given the fact that the flexibility of the membrane may increase the temperature and velocity gradients to capture these gradients adjacent to the boundaries, a clustered grid, assuming symmetric distribution in vertical and horizontal directions in two parts of cavity and element ration to be 0.001, is adopted near the walls and partition. The elemental details of the physical model are presented in Figure 1. Except for density alteration that is conformed to Boussinesq assumption, the other thermophysical properties of the fluid are assumed constant. To model the fluid motion in FSI approach, a Lagrangian–Eulerian formulation is implemented. The unsteady form of the governing equations for mass, momentum and thermal energy in the fluid phase for the partitioned cavity are represented here in canonical forms (Khanafer *et al.*, 2010; Khanafer and Vafai, 2010):

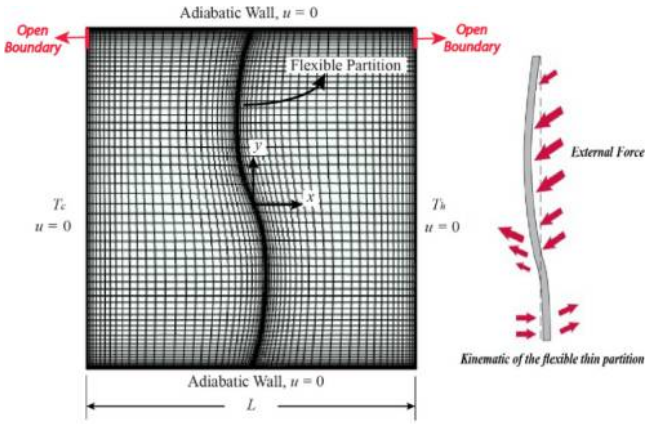

Notes: The open boundaries with a length of 0.1 per cent of cavity wall are assumed to satisfy continuity of mass for an incompressible fluid flow. The structured grid is clustered near the boundaries to capture the essential gradients

Figure 1.
Schematic diagram of the physical model in which the coordinate system is considered to be at the center of enclosure and the membrane is deformed under external forces

$$\nabla \cdot u = 0 \tag{1}$$

$$\frac{\partial u}{\partial \tau} + (u - u_p) \cdot \nabla u = -\nabla \cdot \sigma_f + f_{yi} \tag{2}$$

$$\frac{\partial \theta}{\partial \tau} + (u - u_p) \cdot \nabla \theta = \nabla^2 \theta \tag{3}$$

and quantities are nondimensionalized using the following parameters:

$$\tau = \frac{t\alpha_f}{L^2}\ ,\ (x,y) = \frac{(x^*,y^*)}{L}\ ,\ (u,v) = \frac{(u^*,v^*)L}{\alpha_f}$$
$$p = \frac{P^*L^2}{\rho_f \alpha_f^2}\ ,\ \theta = \frac{T^* - T_0}{T_h - T_c}\ ,\ u_p = \frac{u_p^* L}{\alpha_f} \tag{4}$$

Here, u is velocity vector of fluid; u_p is velocity of moving coordinate; (u-u_p) is relative velocity; θ is nondimensional temperature; τ is nondimensional time; P is dimensionless pressure; σ_f is fluid stress tensor which is equal to $p - \Pr\nabla.u$; $f_{yi} = Pr \times Ra \times \theta$ is dimensionless body force; $Pr = \nu/\alpha_f$ is the Prandtl number; and $Ra = [g\beta(T_h\text{-}T_c)L^3]/\nu\alpha_f$ is Rayleigh number. The initial condition of the working fluid is considered to be quiescent (u (x, y, 0) = 0). Moreover, considering the left and right vertical conditions to be T_c and T_h, respectively, the thin flexible partition temperature is selected to be initially $(T_h+T_c)/2$. Equations (1-3) are subjected to the boundary conditions of equation (5):

$$u = 0\ ,\ \theta = 0.5\ at\ x = 0.5$$
$$u = 0\ ,\ \theta = -0.5\ at\ x = -0.5$$
$$u = 0\ ,\ \frac{\partial \theta}{\partial y} = 0\ at\ y = -0.5\ and\ 0.5 \tag{5}$$

It is assumed that the flexible partition is a simple hyper-elastic material. Therefore, considering the nonlinear geometric effects and using the Neo-Hookean model, the stress tensor σ^* is introduced as equation (6):

$$\sigma^* = J^{-1}FSF^T \tag{6}$$

where $F = \left(I + \nabla d_s^*\right), J = \det(F)$ and S= $\partial W_s/\partial\varepsilon$ in which d_s^* is dimensional displacement of the membrane; Ws is function of strain energy density, and ε denotes strain, which are described as equations (7) and (8):

Table I. Grid independence test for $E_\tau = 1 \times 10^{14}$, $F_V = 0$, $Pr = 5.476$ and different Rayleigh numbers

Grid size	$Ra = 1 \times 10^7$	$Ra = 1 \times 10^8$
60 × 60	8.1465	16.7791
80 × 80	8.1547	16.7883
100 × 100	8.1588	16.7985
120 × 120	8.1596	16.7992
150 × 150	8.1598	16.7998

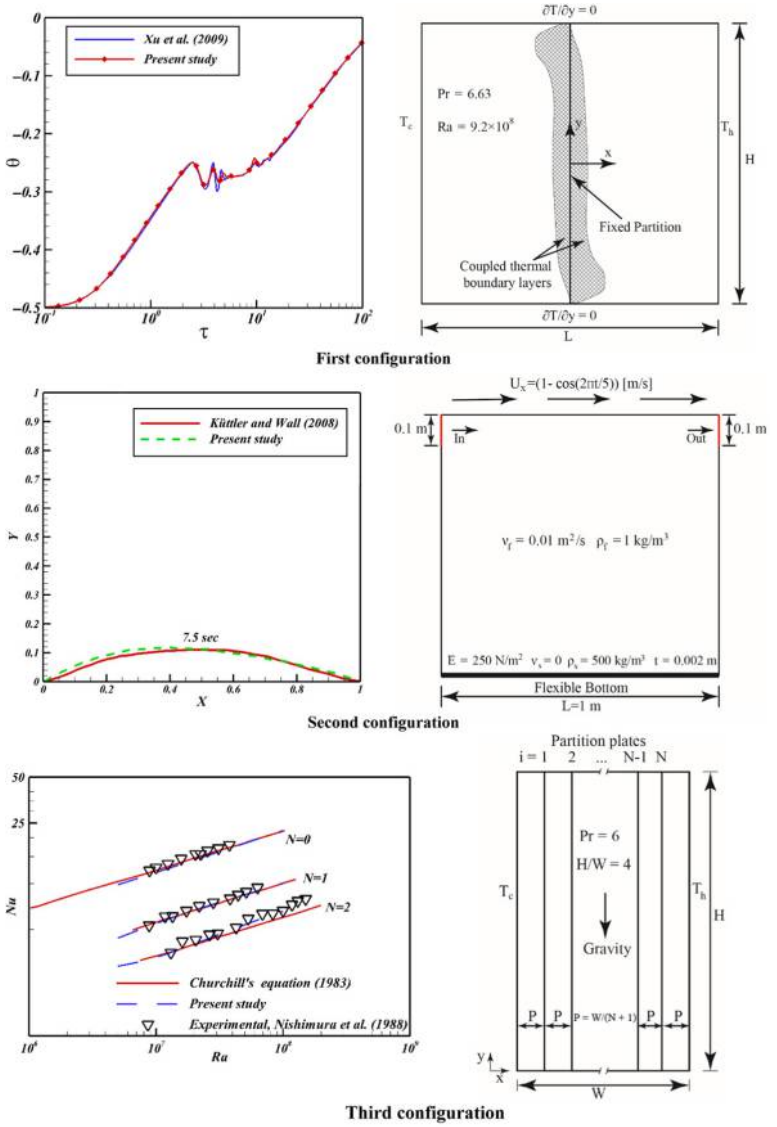

Notes: First configuration: variation of temperatures with time at the point ($x = -0.0083$, $y = 0.375$) on the left side of the middle fixed plate which is in the downstream thermal boundary layer and with $Pr = 6.63$, $Ra = 9.2\times108$ [Xu *et al*., 2009]; second configuration: comparing the deformation of bottom flexible wall with time-dependent upper boundary condition of a lid-driven enclosure at $t = 7.5$ s (Küttler and Wall, 2008); third configuration: comparing the effect of Ra on the Nusselt number for natural convection in a cavity with multiple partitions, $Pr = 6$ and H/W = 4 [Nishimura *et al*. 1988, Churchill 1983]

Figure 2.
Comparing the present results and literature data

$$W_s = \frac{1}{2}\mu_l\left(J^{-1}I_1 - 3\right) - \mu_l \ln(J) + \frac{1}{2}\lambda\left(\ln(J)\right)^2 \tag{7}$$

$$\varepsilon = \frac{1}{2}\left(\nabla d_s^* + \nabla d_s^{*T} + \nabla d_s^{*T}\nabla d_s^*\right) \tag{8}$$

where I_1 is the first invariant of the right Cauchy–Green deformation tensor. The coefficients of μ_l and λ are Lamé parameters calculated as $\mu_l = E/(2(1+\nu))$ and $\lambda = Ev/[(1+v)(1-2v)]$ in which E is Young's modulus and ν is kinematic viscosity. Furthermore, it should be noted that the model of Neo-Hookean is unable for modeling materials such as plastics and rubber-like membranes (Gent, 2001).

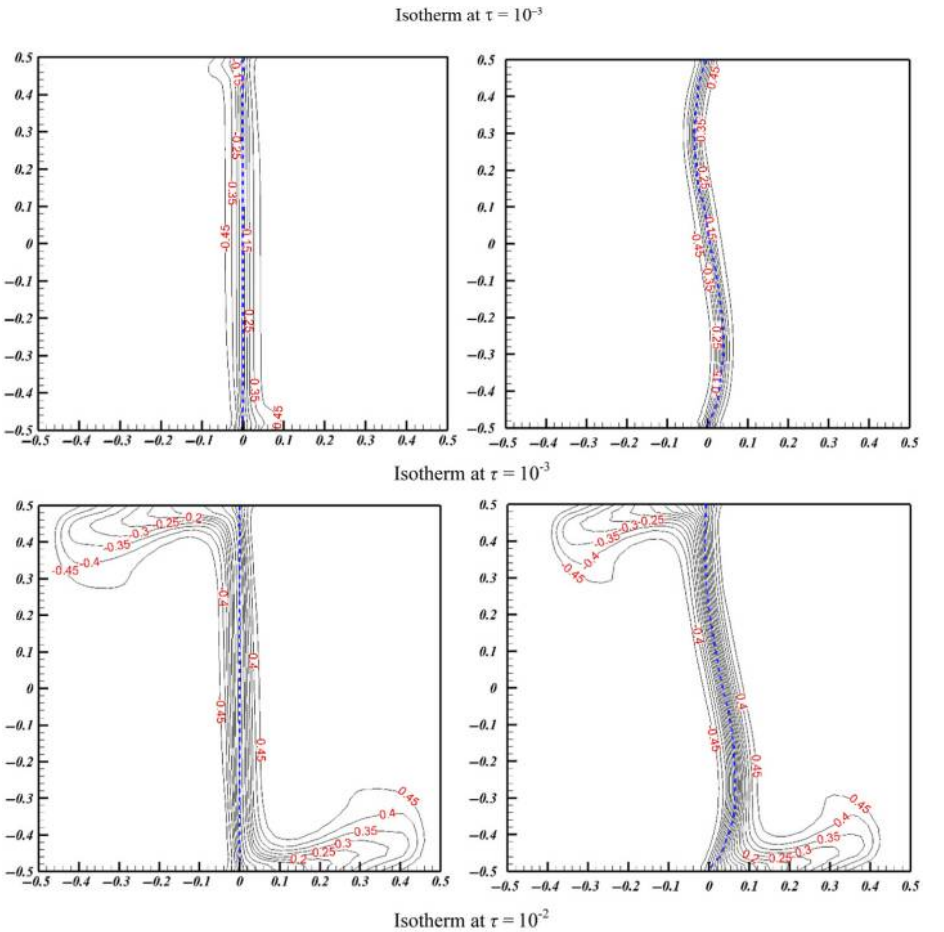

Figure 3.
Comparison of the temperature contours of enclosures with fixed (left side) and flexible (right side) partition at different times with the same boundary conditions

(*continued*)

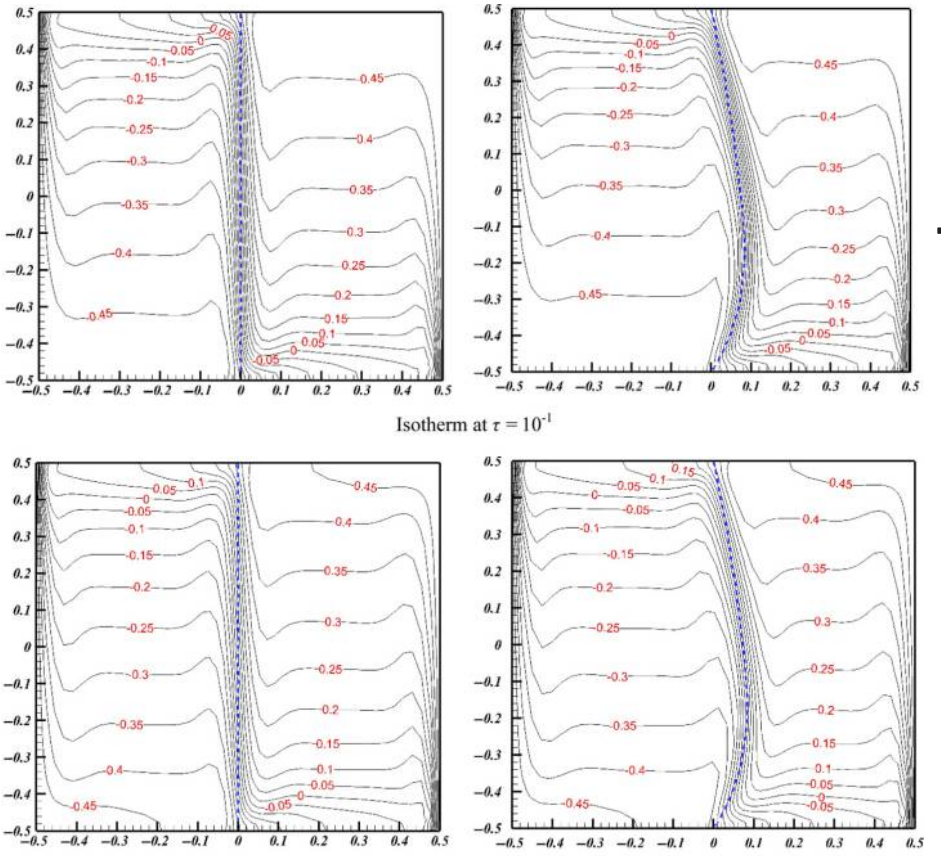

Notes: The thermophysical parameters are defined as $E_\tau = 1 \times 10^{14}$, $F_v = 0$, $Ra = 1.0048 \times 10^7$, $Pr = 5.476$

Figure 3.

The governing equation for the flexible partition domain of the FSI model can be represented by the elasto-dynamics equation (9) (Al-Amiri and Khanafer, 2011; Jamesahar *et al.*, 2016; Khanafer *et al.*, 2010; Khanafer and Vafai, 2010):

$$\frac{1}{\rho_R}\frac{d^2 d_s}{d\tau^2} - E_\tau \nabla \sigma_s = E_\tau F_v \tag{9}$$

where d_s denotes the nondimensional solid displacement vector of the thin flexible partition; F_v is the nondimensional externally applied body force vector at time τ; ρ_R is the ratio of fluid to solid densities; and σ_s is the solid stress tensor introduced as equation (10):

$$E_\tau = \frac{EL^2}{\rho_f \alpha_f^2}\ ,\ F_v = \frac{(\rho_f - \rho_s)Lg_y}{E}\ ,\ \rho_R = \frac{\rho_f}{\rho_s}\ ,\ d_s = \frac{d_s^*}{L}\ ,\ \sigma_s = \frac{\sigma^*}{E} \tag{10}$$

Given the fact that the membrane is highly conductive, balancing energy at the fluid-solid interface leads to an equal temperature gradient. In addition, considering the continuity of dynamic movements and kinematic forces for fluid-solid interaction at the partition surface and no-slip boundary condition, we have:

$$\frac{\partial d_s}{\partial \tau} = u \ , \ E_\tau \sigma . n = -P + \mathrm{Pr} \nabla u \tag{11}$$

3. Method of solution and validation

Using the Galerkin method as a finite-element approach with iteration, the system of governing equations (1-3, 9) along with their boundary conditions, equations (5, 11) are transformed to a weak form and solved numerically. The termination of iteration process

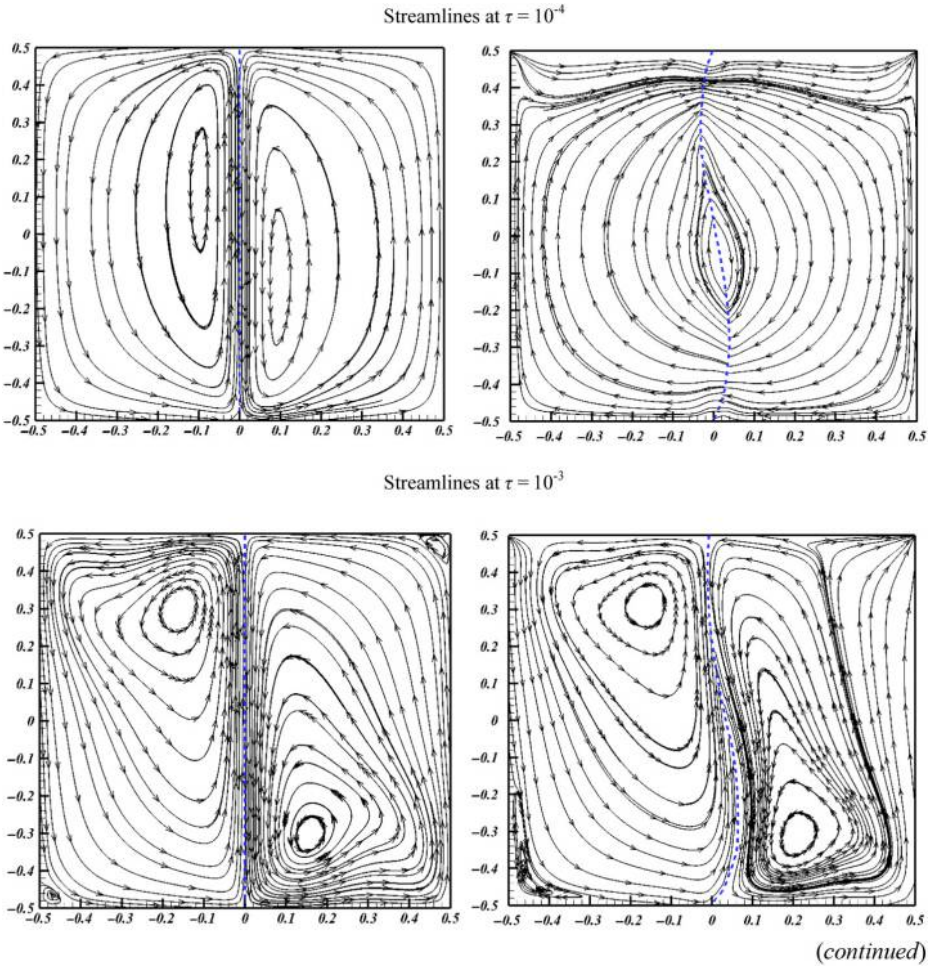

Figure 4.
Comparison of the streamlines of cavity with fixed (left side) and flexible (right side) partitions at different times with the same boundary conditions

(*continued*)

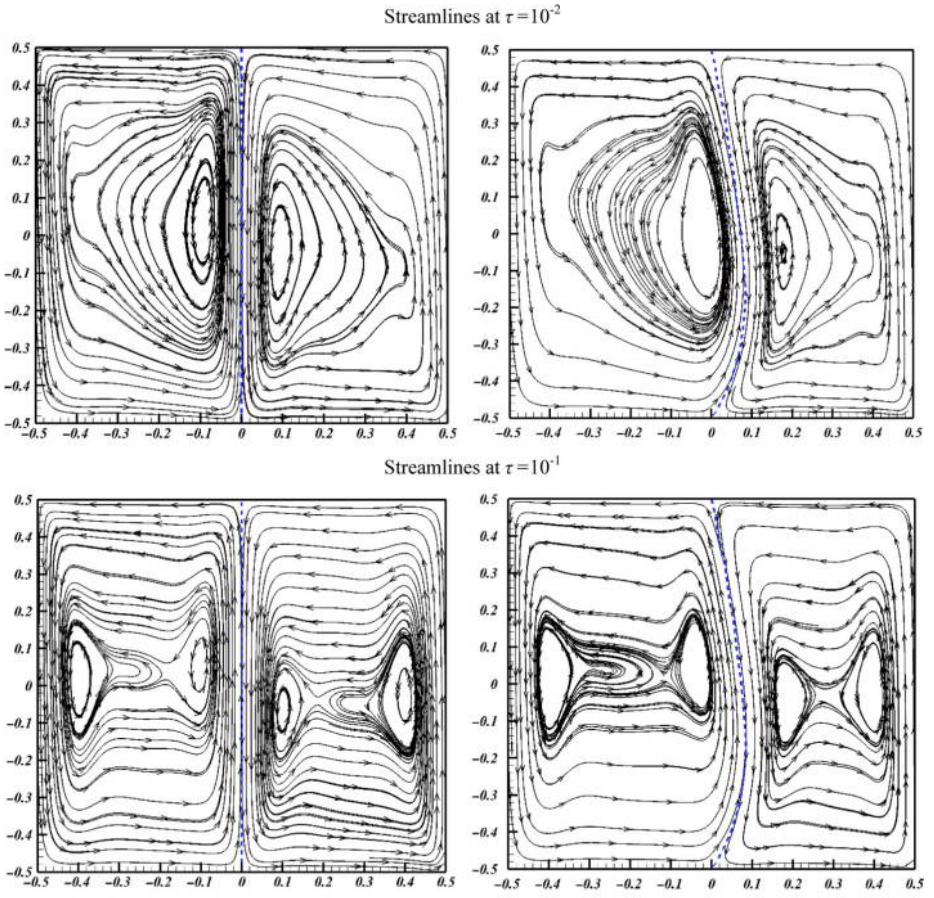

Notes: The thermo-physical parameters are defined as $E_\tau = 1 \times 10^{14}$, $F_v = 0$, $Ra = 1.0048 \times 10^7$, $Pr = 5.476$

Figure 4.

occurs when the residuals for the defined dependent variables become less than 10^{-8}. The meticulous information about solution methods is obtained in the literature (Reddy, 1993; Basak *et al.*, 2006). To ensure that an accurate solution is independent of grid size, the steady state average Nusselt numbers of the left cold wall for different grid sizes and two Rayleigh numbers are calculated (Table I). The grid size of 120 × 120 provides accurate results and used for the simulations in this work.

Three different configurations are modeled to confirm the solution procedure validation. First, a cavity with a centered vertical fixed thin partition with the boundary conditions of equation (5) (Xu *et al.*, 2009); second, a lid driven cavity with a flexible bottom surface (Küttler and Wall, 2008); and third, an experimental study recapitulating the Nishimura *et al.* (1988), work considering natural convection heat transfer in a cavity with multiple vertical partitions. Comparing the results of current research and the works of literature (Figure 2), show an excellent match between the computed temperature, deformation and Nusselt

number in the first, second and third configurations (Xu *et al.*, 2009; Küttler and Wall 2008; Nishimura *et al.*, 1988; Churchill, 1983).

4. Results and discussion

To investigate the unsteady free convection of the enclosure with an elastic vertical partition, placed in the center of geometry, the nondimensional parameters *Ra* and *Pr* are fixed to 1.0048×10^7 and 5.476, respectively. The time step is assumed to be adjustable. The results are presented for a set of nondimensional parameters unless otherwise mentioned.

The temperature contour maps (isotherms) of the cavities with fixed and flexible partitions at different times are presented in Figure 3. According to the isotherms for rigid partition model and FSI model in different times (Figure 3), the heat transfer is augmented when the middle partition is deformed. According to the present results, the shape of the flexible partition is profoundly dependent on the time.

Increasing the time induces an elevation in the convection heat transfer which leads to augmentation of the external force and consequently soaring the flexible partition deformation. In addition, the deformation of flexible partition changes the flow regime and consequently temperature distribution. Moreover, the streamlines corresponding to the presented isotherms (Figure 3) are shown in Figure 4. The streamlines develop with time and the deformation of the flexible thin partition affects the pressure distribution in the domain; consequently, it leads to elongating the recirculation region of the flow on both sides of the partition and therefore influences the heat transfer in the cavity.

The displacement of the elastic thin partition over time at two points ($x = 0, y = 0.25$) and ($x = 0, y = -0.25$) is evaluated (Figure 5). The results show that the deflections at the top and bottom parts of the partition change smoothly at beginning followed by fluctuating over time, and finally, it becomes constant in the steady state condition. Generally, the displacement is an increasing function of time at beginning as the heat transfer and fluid flow empower the external forces. The oscillation of the flexible partition then dwindles slightly as the partition deformation reaches to an almost steady form. Further, the fluctuation in the vertical direction is negligible

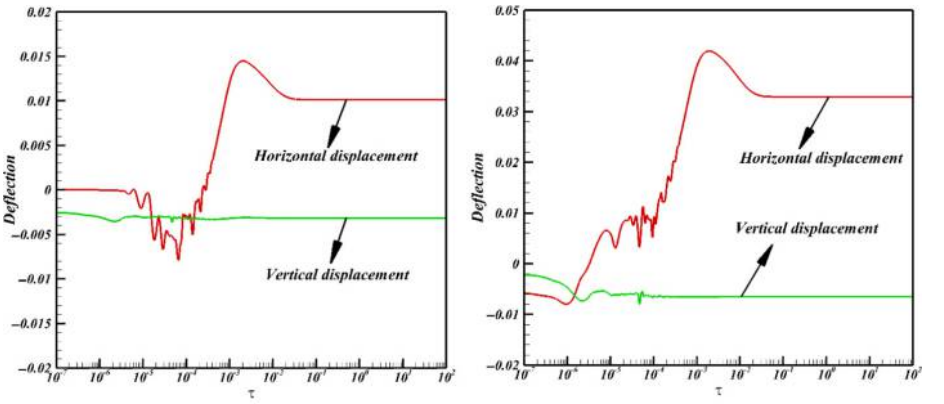

Figure 5.
The horizontal and vertical deflection of the two points of the flexible partition over time

Notes: Left side (0,0.25) located at the upper part of the membrane, and right side (0,–0.25) located at the bottom part of the membrane with $E_\tau = 1.4 \times 10^{15}$, $F_v = -0.016$, $Ra = 1.0048 \times 10^7$, $Pr = 5.476$

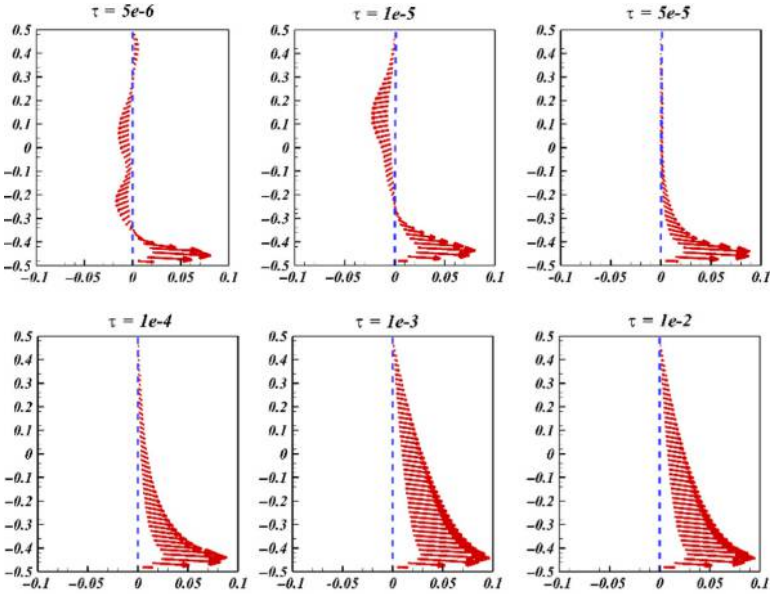

Notes: The membrane is noticeably oscillated at early times and then its deformation reaches gradually to a fixed shape

Figure 6.
Total deformation of the flexible thin partition for different times, $E_\tau = 1 \times 10^{14}$, $F_V = -1.646 \times 10^{-2}$, $Ra = 1.0048 \times 10^7$, $Pr = 5.476$

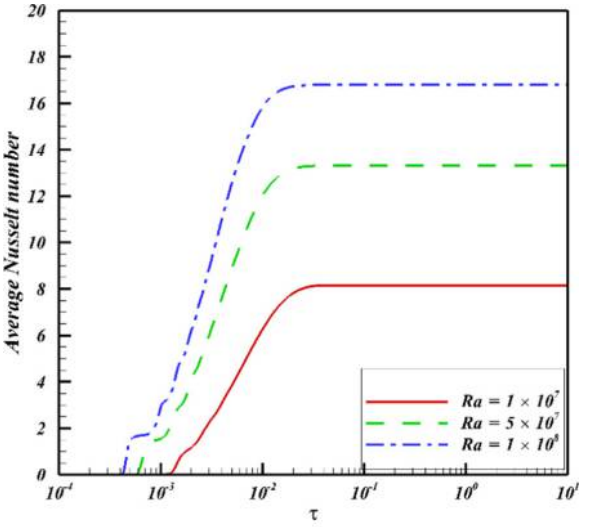

Notes: The $\overline{Nu}$ is an increasing function of the Ra. As time goes on, the $\overline{Nu}$ ascends and then reaches a steady state value

Figure 7.
Variation of the average Nusselt number of the left vertical boundary with time for different Rayleigh numbers, $E_\tau = 1 \times 10^{14}$, $F_V = 0$, $Pr = 5.476$

with respect to the horizontal direction. Also, the displacement of the thin membrane is drastically affected by the physical and thermophysical properties. Figure 5 shows the general behavior of the flexible partition respect to time for two target points.

The displacement of the thin flexible partition respect to time is shown in Figure 6. As substantiated in Figure 6, in contrast to the lower and upper part of the thin flexible partition, the most part of the membrane is deformed and vibrated to the left side of the initial position at beginning ($\tau = 5 \times 10^{-6}$). Moreover, as time goes on, the membrane deflection leans right. Owing to the fact that the fluid flow circulation in right compartment is in the opposite direction to the left one, the external forces applied to the centered thin partition change proportional to the fluid flow regime. In addition, the deformation becomes almost invariant at $\tau = 10^{-3}$.

The effect of Rayleigh number on the average Nusselt number on the left cold wall is shown in Figure 7. The results show that when the Rayleigh number increases, the value of average Nusselt number ascends significantly. Moreover, decrease in Rayleigh number reduces period of reaching to steady state condition. As time goes on, the difference between the average Nusselt numbers for various Rayleigh numbers soars and it continues to reach a steady state condition under which the difference remains constant.

Moreover, calculating the maximum nondimensional stress in the membrane is critical for evaluating the heat and mass transfer. The variation of stress for various Young's modulus and Rayleigh numbers is shown in Figure 8. The stress is an increasing function of E_τ and depending upon the value of the Ra, this increment function shows a different behavior. For instance, the slope of the increase in stress for $Ra = 1.0048 \times 10^7$ is low and as E_τ ascends, this slope becomes higher and reaches a constant value. On the other hand, the stress increases by increasing E_τ with a constant rate for $Ra = 1.0048 \times 10^5$. Also, any increase in the modulus of elasticity leads to an increase in the stiffness of the membrane and the value of stress. Furthermore, increasing the magnitude of Rayleigh number

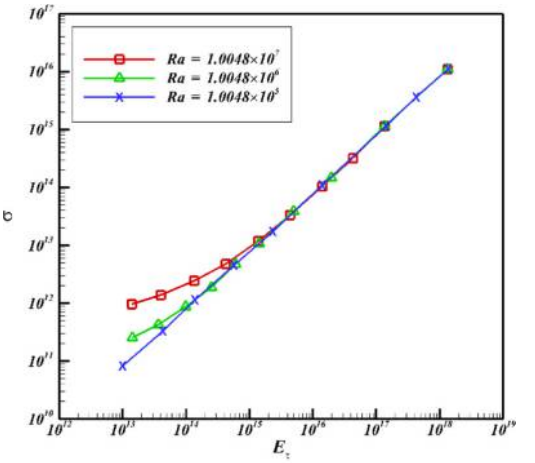

Notes: The more increase in E_τ, the more increase in σ. The parameter σ elevates by increasing Ra for low E_τ values and it becomes independent from Ra for high E_τ values

Figure 8.
The dimensionless stress of the flexible partition as a function of different dimensionless Young's modulus values and different Rayleigh numbers, $F_V = -1.646 \times 10^{-2}$, $Pr = 5.476$

increases the stress for low values of E_τ. On the other hand, for high values of E_τ, the variation of Rayleigh number has no effect on the stress. In fact, the alteration in stress resulted from changes in Rayleigh number is due to the effect of buoyancy force on the flexible partition. Accordingly, as the modulus of elasticity increases, the augmentation of stiffness dominates the variation of buoyancy force.

The variation of dimensionless stress and deformation of the flexible partition in the steady state under different body forces applied on the membrane is represented in Figure 9.

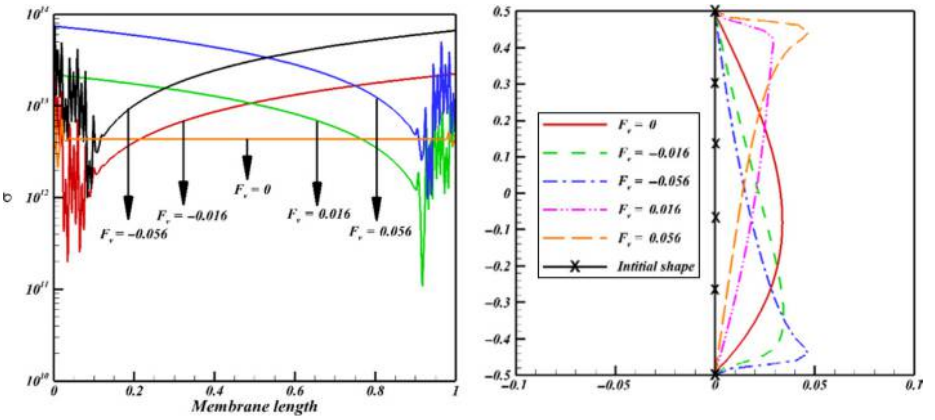

Notes: The more increase in F_v value, the more increase in σ. Right side: deformation of the membrane in steady state, the profound effect of F_v value on the final deformation of the flexible partition

Figure 9. The effect of applied nondimensional body force on the membrane for $E_\tau = 1 \times 10^{15}$, $Ra = 1.0048 \times 10^7$, $Pr = 5.476$, left side: variation of nondimensional stress in the steady state

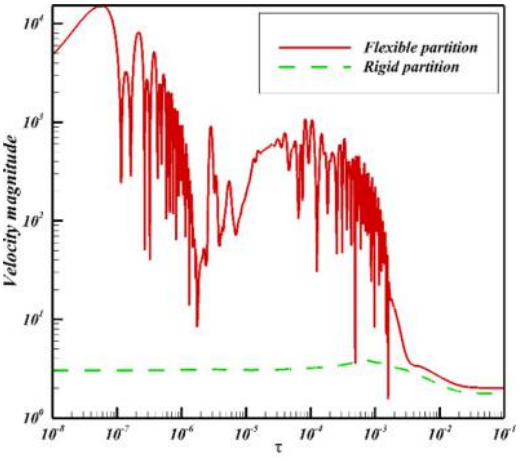

Notes: Higher magnitude of the velocity adjacent to the flexible partition respect to the fixed membrane is obvious at early times

Figure 10. Comparing the alteration of velocity magnitudes with nondimensional time at point (0.25, 0), the upper part of the membrane, between the square enclosures with flexible and rigid partitions for $E_\tau = 1 \times 10^{14}$, $F_V = 0$, $Ra = 1.0048 \times 10^7$, $Pr = 5.476$

Depending on the value of the applied body forces, the steady state stress of the membrane varies. In other words, in the case of $F_v = 0$, the stress remains approximately constant. In addition, when the applied body force is negative, the stress at the bottom of the membrane fluctuates and then soars when the membrane length is approximately greater than 0.1. On the contrary, for the positive values of F_v, the fluctuation phenomenon occurs on the top section of the membrane and the stress increases when the membrane length becomes less than 0.9. Moreover, the shape of the deformed membrane in the steady state, which is dependent on the stress, is variable (Figure 9). In other words, the maximum deflection of the membrane in positive and negative values of the applied force take place on top and bottom sections of the flexible partition, respectively. Noted that, the more increase in the value of F_v, the more increase in the magnitude of the stress and deformation.

It is worth mentioning that the variation of parameters such as Prandtl number, Young's modulus and applied body force on the membrane do not have noticeable impact on the heat transfer; therefore, the effect of these parameters on the Nusselt number has not been shown here, for the sake of brevity.

Finally, to find out the influence of flexible thin partition on velocity field, the velocity magnitude at point (0.25, 0) over time is shown in Figure 10. The results show that the velocity value fluctuation is profoundly reflected by the deformation of the flexible thin partition. In other words, there is a significant difference between the point velocities magnitudes in cavities with rigid and flexible partitions at early times, for which the flexible partition fluctuates noticeably.

5. Conclusion

The transient natural convection of an enclosure with a hyper-elastic thin partition is numerically investigated. The diathermal membrane is vertically located at the center of the enclosure with a zero thickness and infinite conductivity, under which only the heat transfer perpendicular to the flexible partition is modeled. The effect of both flexible and rigid thin partition with the cavity on the heat transfer are investigated and compared. Moreover, the influence of Rayleigh number on the average Nusselt number of the left vertical wall is evaluated. The maximum and steady state nondimensional stress under various parameters of the system are calculated. The heat transfer in a flexible partition in a nutshell augments with respect to a rigid partition. Furthermore, the higher the Rayleigh number, the higher the average Nusselt number of the left vertical wall. As Rayleigh number dwindles, the period of reaching the steady state condition decreases. Furthermore, as the modulus of elasticity increases, the maximum nondimensional stress soars significantly. When the value of modulus of elasticity is low, increasing of Rayleigh number leads to an increase in the maximum nondimensional stress. In addition, depending on the value of applied body force on the membrane, the dimensionless steady state stress and deformation in the flexible partition are variable. Finally, it is concluded that the deflection of the membrane leans right in the steady state due to external forces of the flow field.

References

Al-Amiri, A. and Khanafer, K. (2011), "Fluid–structure interaction analysis of mixed convection heat transfer in a lid-driven cavity with a flexible bottom wall", *International Journal of Heat and Mass Transfer*, Vol. 54 Nos 17/18, pp. 3826-3836.

Basak, T., Roy, S., Paul, T. and Pop, I. (2006), "Natural convection in a square cavity filled with a porous medium: effects of various thermal boundary conditions", *International Journal of Heat and Mass Transfer*, Vol. 49 Nos 7/8, pp. 1430-1441.

Chamkha, A.J., Hussain, S.H., Ali, F.H. and Shaker, A.A. (2012), "Conduction-combined forced and natural convection in a lid-driven parallelogram-shaped enclosure divided by a solid partition", *Progress in Computational Fluid Dynamics, an International Journal*, Vol. 12 No. 5, pp. 309-321.

Churchill, S.W. (1983), "Free convection in layers and enclosures", *Heat Exchanger Design Handbook*, Hemisphere Publishing Corporation, New York, NY.

Cuckovic-Dzodzo, D.M., Dzodzo, M.B. and Pavlovic, M.D. (1999), "Laminar natural convection in a fully partitioned enclosure containing fluid with nonlinear thermophysical properties", *International Journal of Heat and Fluid Flow*, Vol. 20 No. 6, pp. 614-623.

Duxbury, D. (1979), "An interferometric study of natural convection in enclosed plane air layers with complete and partial central vertical divisions", Ph.D. Thesis, University of Salford, Greater Manchester.

Gent, A.N. (Ed.) (2001), *Engineering with Rubber*, Carl Hanser Verlag, Munich, Germany.

Jamesahar, E., Ghalambaz, M. and Chamkha, A.J. (2016), "Fluid–solid interaction in natural convection heat transfer in a square cavity with a perfectly thermal-conductive flexible diagonal partition", *International Journal of Heat and Mass Transfer*, Vol. 100, pp. 303-319.

Khaled, A.R.A. and Vafai, K. (2002), "Flow and heat transfer inside thin films supported by soft seals in the presence of internal and external pressure pulsations", *International Journal of Heat and Mass Transfer*, Vol. 45 No. 26, pp. 5107-5115.

Khaled, A.R.A. and Vafai, K. (2003), "Analysis of flow and heat transfer inside oscillatory squeezed thin films subject to a varying clearance", *International Journal of Heat and Mass Transfer*, Vol. 46 No. 4, pp. 631-641.

Khanafer, K. and Vafai, K. (2010), "Microcantilevers in biomedical and thermo/fluid applications", *Frontiers in Heat and Mass Transfer*, Vol. 1 No. 2, p. 023004.

Khanafer, K., Alamiri, A. and Pop, I. (2010), "Fluid–structure interaction analysis of flow and heat transfer characteristics around a flexible microcantilever in a fluidic cell", *International Journal of Heat and Mass Transfer*, Vol. 53 Nos 9/10, pp. 1646-1653.

Küttler, U. and Wall, W.A. (2008), "Fixed-point fluid–structure interaction solvers with dynamic relaxation", *Computational Mechanics*, Vol. 43 No. 1, pp. 61-72.

Martyushev, S.G. and Sheremet, M.A. (2014), "Conjugate natural convection combined with surface thermal radiation in an air filled cavity with internal heat source", *International Journal of Thermal Sciences*, Vol. 76, pp. 51-67.

Mehryan, S.A.M., Ghalambaz, M., Ismael, M.A. and Chamkha, A.J. (2017), "Analysis of fluid- solid interaction in MHD natural convection in a square cavity equally partitioned by a vertical flexible membrane", *Journal of Magnetism and Magnetic Materials*, Vol. 424, pp. 161-173.

Nakamura, M., Nakamura, T. and Tanaka, T.A. (2000), "computational study of viscous flow in a transversely oscillating channel", *JSME International Journal Series C*, Vol. 43 No. 4, pp. 837-844.

Nakamura, M., Sugawara, M. and Kozuka, M. (2001), "Heat transfer characteristics in a two-dimensional channel with oscillating wall", *Heat Transfer?Asian Research*, Vol. 30 No. 4, pp. 280-292.

Nishimura, T., Shiraishi, M., Nagasawa, F. and Kawamura, Y. (1988), "Natural convection heat transfer in enclosures with multiple vertical partitions", *International Journal of Heat and Mass Transfer*, Vol. 31 No. 8, pp. 1679-1686.

Ralph, M.E. and Pedley, T.J. (1988), "Flow in a channel with moving indentation", *Journal of Fluid Mechanics*, Vol. 190 No. 1, pp. 87-112.

Reddy, J.N. (1993), *An Introduction to the Finite Element Method*, McGraw-Hill, New York, NY.

Saha, S.C. and Gu, Y.T. (2014), "Transient air flow and heat transfer in a triangular enclosure with a conducting partition", *Applied Mathematical Modelling*, Vol. 38 Nos 15/16, pp. 3879-3887.

Saha, S.C., Khan, M.M.K. and Gu, Y.T. (2014), "Unsteady buoyancy driven flows and heat transfer through coupled thermal boundary layers in a partitioned triangular enclosure", *International Journal of Heat and Mass Transfer*, Vol. 68, pp. 375-382.

Sathiyamoorthy, M. and Chamkha, A.J. (2014), "Analysis of natural convection in a square cavity with a thin partition for linearly heated side walls", *International Journal of Numerical Methods for Heat and Fluid Flow*, Vol. 24 No. 5, pp. 1057-1072.

Sheikholeslami, M. and Rashidi, M.M. (2015), "Effect of space dependent magnetic field on free convection of Fe3O4–water nanofluid", *J. Taiwan Institute Chemical Engineers*, Vol. 56, pp. 6-15.

Sheikholeslami, M. and Shamlooei, M. (2017), "Fe 3 O 4–H 2 O nanofluid natural convection in presence of thermal radiation", *International Journal of Hydrogen Energy*, Vol. 42 No. 9, pp. 5708-5718.

Sheikholeslami, M. and Shehzad, S.A. (2017a), "Thermal radiation of ferrofluid in existence of Iorentz forces considering variable viscosity", *International Journal of Heat and Mass Transfer*, Vol. 109, pp. 82-92.

Sheikholeslami, M. and Shehzad, S.A. (2017b), "Magnetohydrodynamic nanofluid convection in a porous enclosure considering heat flux boundary condition", *International Journal of Heat and Mass Transfer*, Vol. 106, pp. 1261-1269.

Sheikholeslami, M., Hayat, T. and Alsaedi, A. (2017), "Numerical study for external magnetic source influence on water based nanofluid convective heat transfer", *International Journal of Heat and Mass Transfer*, Vol. 106, pp. 745-755.

Sheremet, M.A. and Pop, I. (2014), "Conjugate natural convection in a square porous cavity filled by a nanofluid using Buongiorno's mathematical model", *International Journal of Heat and Mass Transfer*, Vol. 79, pp. 137-145.

Sheremet, M.A. and Pop, I. (2015), "Natural convection in a wavy porous cavity with sinusoidal temperature distributions on both side walls filled with a nanofluid: Buongiorno's mathematical model", *Journal of Heat Transfer*, Vol. 137 No. 7, p. 072601.

Sheremet, M.A., Grosan, T. and Pop, I. (2015), "Free convection in a square cavity filled with a porous medium saturated by nanofluid using Tiwari and Das' nanofluid model", *Transport in Porous Media*, Vol. 106 No. 3, pp. 595-610.

Xu, F., Patterson, J.C. and Lei, C. (2009), "Heat transfer through coupled thermal boundary layers induced by a suddenly generated temperature difference", *International Journal of Heat and Mass Transfer*, Vol. 52 Nos 21/22, pp. 4966-4975.

Corresponding author
Ioan Pop can be contacted at: popm.ioan@yahoo.co.uk